Mon. Not. R. astr. Soc. (1980) **193**, 645–666

Flux of optical meteors down to $M_{pg} = +12$

A. F. Cook, T. C. Weekes and J. T. Williams
Harvard–Smithsonian Center for Astrophysics, 60 Garden Street, Cambridge, Massachusetts 02138, USA
E. O'Mongain *Physics Department, University College, Dublin, Ireland*

Received 1980 March 17; in original form 1978 January 9

Summary. Observations of meteors, using the 10-m optical reflector on Mt Hopkins in southern Arizona are reported. The observations were made on four successive nights 1974 December during the peak of the Geminid shower. Since the shower made a negligible contribution to the meteor counting rate (2–6 per minute), it was possible, based on the observation of 2222 meteors, to derive a cumulative flux–density relationship of sporadic meteors:

$$\log \phi = -17.88 + 0.533\, M_{pg} \pm 0.40 \pm 0.004$$

where ϕ is the flux in meteors $cm^{-2}\, s^{-1}$ and M_{pg} is the photographic absolute magnitude. This measurement applies over the range $M_{pg} = +7$ to $+12$.

We combine our results with counts of photographic meteors versus maximum absolute magnitude by Hawkins & Upton [1] over the range $-2.4 \leqslant M_{pg} \leqslant +1.6$ to establish a distribution over a wide range of magnitudes:

$$\log \phi = -17.89 + 0.534\, M_{pg} \pm 0.05 \pm 0.004$$

where ϕ is cumulative flux into the atmosphere in $cm^{-2}\, s^{-1}$ of meteors brighter than or as bright as photographic absolute magnitude, M_{pg} (standard range 100 km) at maximum light. Comparisons with other observations by low-light television techniques cover the intermediate range $+1.6 \leqslant M_{pg} \leqslant +7$ and lead to the startling conclusion that this linear relation prevails through the range $-2.4 \leqslant M_{pg} \leqslant +12.0$.

The cumulative flux upon the Earth's atmosphere is estimated at

$$\log \phi_{m\infty} = -17.8 - 1.335 \log m_{\infty} \pm 0.6 \pm 0.010$$

where $\phi_{m\infty}$ is the cumulative flux of all masses, m_∞, and larger in $cm^{-2}\,s^{-1}$, mass, m_∞, being reckoned in grammes. The cumulative flux on a test surface at 1 AU from the Sun and far from the Earth's gravitational field is estimated at

$$\log \phi_{mG} = -18.2 - 1.335 \log m_\infty \\ \pm 0.4 \pm 0.010$$

and the cumulative number density of particles is estimated at

$$\log N_{mG} = -23.8 - 1.335 \log m_\infty, \\ \pm 0.8 \pm 0.010$$

all valid in the range of logarithm of mass

$$-4.4 \quad 1.0 \quad 1.4.$$

The uncertainty in the mass-scale is about ± 0.5 in the logarithm and is dominated by the uncertainty in the distribution of meteors over velocity.

1 Introduction

Optical observations of faint meteors are difficult because of the sporadic nature of the events in the atmosphere, and the relatively large spatial extent of the trails. Thus, although the light intensity is large compared with that from astronomical objects, astronomical techniques cannot readily be applied to meteor detection. Schmidt cameras can detect meteors down to photographic magnitude +4; television systems e.g. SEC Vidicons can extend this limit to +8 but there is some uncertainty in the interpretation of these techniques for the fainter meteors since selection effects must be taken into account. Fainter meteors can be detected using radar techniques but again interpretation is a problem as it affects calibration between the optical and radio techniques.

In this paper we describe the first optical observations of meteors down to a limiting photographic magnitude of +12. The meteors were detected by photometry using a 10-m optical reflector. Although the field of view of the system (1° full diameter of half maximum) was small compared with that usually used in meteor studies, it is large by astronomical standards and was sufficient to detect meteors at a rate of in excess of $300\,hr^{-1}$.

2 Detection system

All the observations reported here were made with the 10-m optical reflector on Mt Hopkins (altitude 2.3 km). The reflector consists of 248 hexagonal front-aluminized mirrors, each of focal length 7.3 m; the mirrors are mounted on a tubular metal frame so that 90 per cent of the light from a distant point source on axis falls within a circle of diameter 5 cm in the focal plane. The reflector is mounted on an alt-azimuth antenna positioner which can be pointed in any direction with a pointing accuracy of 3 arcmin; by means of a previously prepared paper tape, the mount can be set to track sidereally to within 10 arcmin.

The reflector was built in 1968 for a programme of observations of high-energy gamma rays using the atmospheric Cerenkov technique [2]. The mirrors were recoated in 1972; since the reflector is unprotected, the reflectivity gradually decays from the optimum 90 per cent. It is estimated that the reflectivity was about 70 per cent when these observations were made.

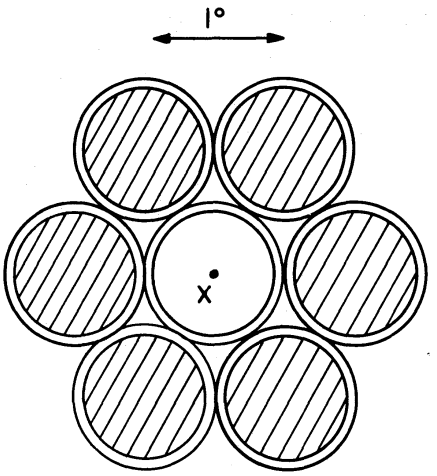

Figure 1. Phototube configuration at focal point of the 10-m reflector. X = detector. Separation between tube centres is 1°.2. Cross-hatched areas are covered by guard ring.

The gamma ray observations are made using a 12.5-cm phototube (RCA 4522) which subtends a 1° full field on the reflector and has a high quantum efficiency in the range 3000–4500 Å. The same tube was used for the meteor observations. The central tube (the detector) was surrounded by a ring of six similar phototubes (the guard ring), whose centres were at a distance of 1°.2 from centre of the detector. This distance was dictated by the diameter of the magnetic shields (15 cm) (Fig. 1).

Each of the seven tubes had a separate high voltage supply; their outputs were taken through 170 m of high grade coaxial cable to the control room where the signals were processed. The detector signal was divided and direct coupled to two amplifiers which had high frequency cut-offs of 10 and 100 Hz respectively. The two bandwidths were used to optimize the signal-to-noise for event selection. The high frequency cut-off was chosen to eliminate the 120 Hz signal from scattered man-made light which is significant even at a dark astronomical site such as Mt Hopkins. The amplifier output was divided and displayed on two channels (A and B) of a fast six pen chart recorder; channel B had a 20 dB attenuator in series so that a total dynamic range of 10^2 was covered. The gain on channel A was set such that noise was about 3 per cent of the full scale deflection. The output of the 10 Hz amplifier was displayed on channel C of the recorder (Fig. 2).

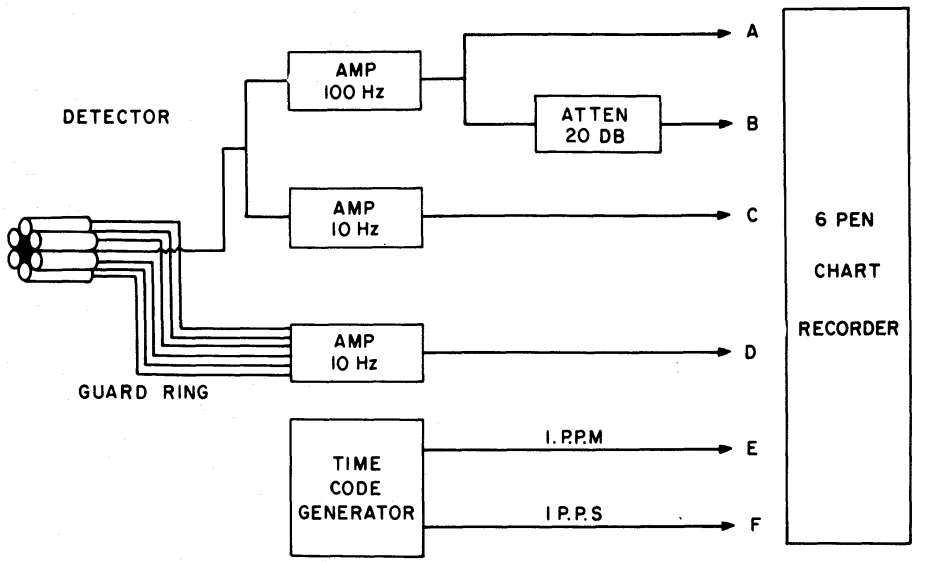

Figure 2. Block diagram of recording system.

The gains of the six guard ring tubes were adjusted so each gave the same output when equally illuminated by a pulsed light emitting diode (LED) source at the centre of the reflector; the six outputs were then added, amplified (bandwidth dc to 10 Hz) and displayed on channel D of the recorder. The chart was run at 2.5 cm s^{-1} and time signals (one pulse per second and one pulse per minute) were displayed on the remaining channels of the recorder. Since the amplifiers were direct coupled, it was necessary to adjust manually the zero level if the background current from the night-sky varied. The noise level was significantly lower when a region of dark sky (relatively free of bright stars) was tracked than when the reflector was kept fixed (in which case the stellar background changed with the Earth's rotation).

3 Observations and analysis

All of the observations were made on the nights of 1974 December 12–15 between $8^h\,0^m$ and $12^h\,0^m$ UT. The weather was clear throughout this period although some thin cirrus was observed towards the end of the observations on December 13. The observations were not continuous but were in runs of 40 min duration with a 5–10 min interval between runs. All of the observations were made with the 10-m reflector in a sidereally tracking mode; the reflector was directed throughout at a point within 1° of the radiant of the Geminid shower which was expected to peak on December 14.

The observed meteor rate was from 2 to 6 min^{-1} where the threshold was defined to be such that the events were clearly identifiable above noise.

During these observations the Vidicon system developed by Clifton [3] was operated at the same site making independent spectroscopic observations of brighter members of the Geminid shower.

The data were analysed by first dividing the six channel chart records into 5 min segments. These were then selected at random by a scanner who recorded the characteristics of each meteor pulse. The parameters recorded were (1) time of arrival (2) the maximum pulse height in the A or B channel (3) the width at half-maximum (4) the area (5) the rise time (6) the fall time (7) the height and width of the pulse (if any) in the guard ring and its offset in time both before and after the detector pulse.

Meteors were most easily identified on the detector A channel which was used as the event selector. Any pulse on that channel that was more than two scale divisions high (Fig. 3) was selected; near the threshold this had the effect of biassing in favour of short duration events (< 40 ms) since these were most obvious as distinct pulses. At very low elevations, the background light noise level increased so that the effective threshold for meteor detection was a factor of 2 higher than normal. In general these observations were not included in the analysis.

4 Sensitivity

4.1 DETECTOR CALIBRATION

A relatively simple calibration procedure was used to determine the peak pulse height in terms of stellar magnitudes of A0 stars without correction for atmospheric extinction.

The 10-m reflector was oriented to point at a bright A0 star ($m_v \sim +3$) in a relatively isolated part of the sky and the increase in current in the detector phototube due to the star was noted. With the reflector pointing to a typical dark region of sky a filament lamp, which was mounted so that it was visible to the detector tube, was adjusted to give the same current as that star of known magnitude. The lamp was then covered by neutral density

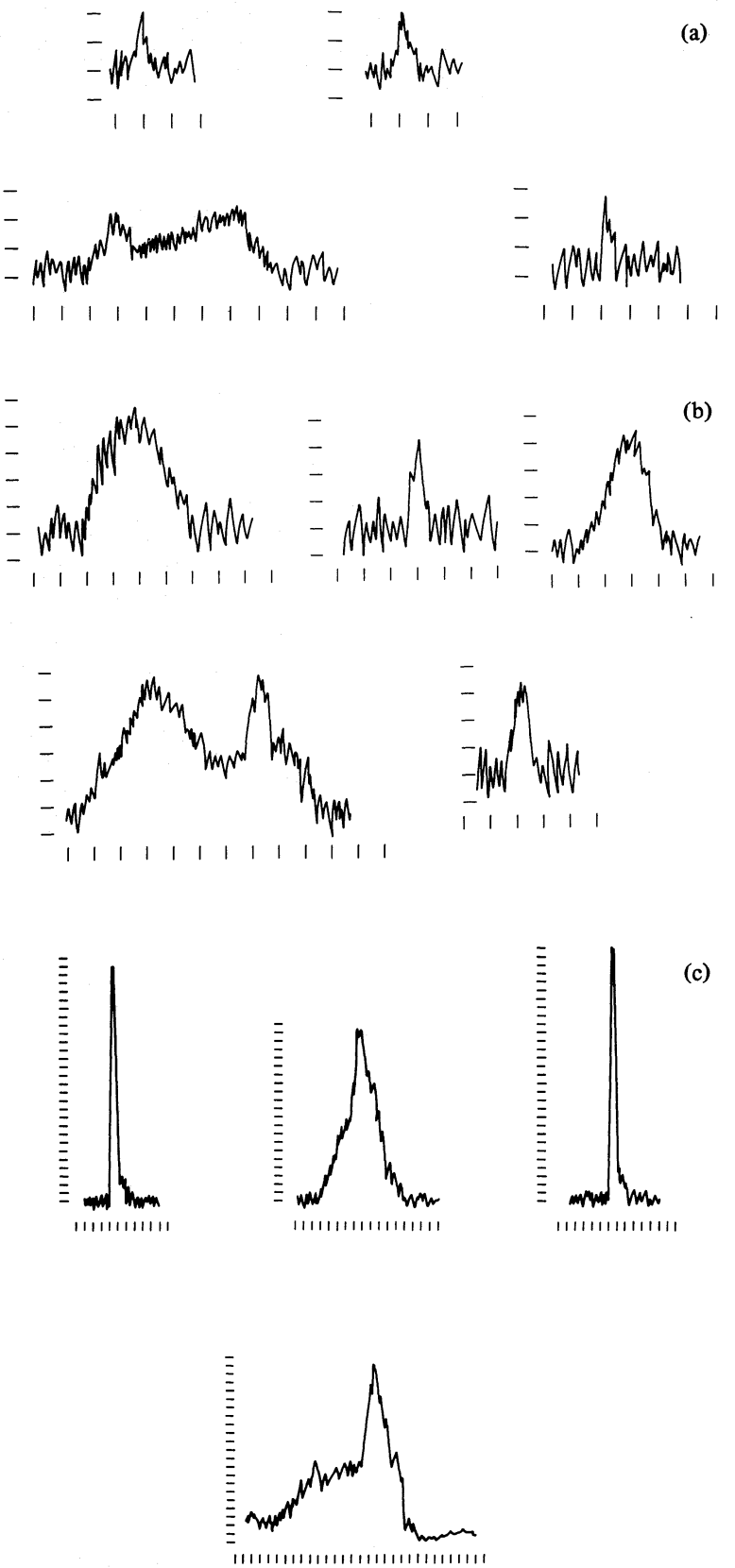

Figure 3. Examples of light pulses detected from meteors on channel A. Vertical divisions correspond to chart divisions where two divisions were taken as threshold. One horizontal division = 40 ms. (a) Examples of events which were just above threshold ($m_{pg} \sim +12$), (b) a selection of pulses of varying shape, (c) larger pulses.

filters; these were increased in density until the signal from the lamp, modulated by a chopping wheel, was just detectable above the background night sky noise i.e. two divisions on the chart record. The threshold for pulse detection, P_T is then given by

$$P_T = M + N,$$

where M = magnitude of the A0 star and N = neutral density factor in stellar magnitudes.

Using this technique, we found $P_T = +12.0\, m_v \sim +12.0\, m_{pg}$ with an estimated uncertainty of ± 0.7 mag the colour of an A0 star being taken to be $m_{pg} - m_v = 0.0$ mag.

4.2 GUARD RING CALIBRATION

The guard ring was primarily intended to act as a veto and to enable the selection of meteors from the Geminid shower radiant which travelled parallel to the reflector axis. The phototube with the highest quantum efficiency was used in the detector channel; the six tubes which constituted the guard ring were on average a factor of 2 less efficient than the detector. Also since the outputs of the six tubes were added, the signal-to-noise ratio was reduced by a factor of $\sqrt{6}$; the result was that the guard ring was a factor of 5–6 times less efficient than the detector at detecting meteors. In addition, the Gaussian-like angular response of the detectors and physical separation between the detectors complicates the interpretation of the guard ring signals.

The sensivity of the individual guard ring channels was measured relative to the detector channel using a pulsed LED. Throughout the observations the LED was pulsed at one minute intervals and the relative responses of the detector and the guard ring monitored.

4.3 SENSITIVITY ESTIMATE

The sensitivity of the detector channel to optical meteors of 20 ms duration can be estimated assuming that the light fluctuations in the sky background are only statistical.

The detectable signal at the 10σ level is given by:

$$S = 10\left(\frac{B_\lambda \Delta\lambda Q \Omega A R T}{h\nu}\right)^{1/2}$$

where

B_λ = background light = 1.7×10^{-7} erg cm^{-2} s^{-1} Å^{-1} [4],
$\Delta\lambda$ = effective bandwidth = 1500 Å,
Q = quantum efficiency = 0.20 from 3000 to 4500 Å,
Ω = field of view = 2×10^{-4} sr,
A = mirror area = 75 m^2,
R = mirror reflectivity = 0.7,
$h\nu$ = effective photon energy = 4.8×10^{-12} erg,
T = resolving time = 20 ms.

We find $S = 4.7 \times 10^4$ photoelectrons/resolving time. This corresponds to an optical flux of 0.31 photons cm^{-2} s^{-1} or 2.5×10^{-14} erg cm^{-2} s^{-1} Å^{-1}. Using the expression $\log f_\lambda(B) = -0.4\, m_B - 8.21$ [4], we get $m_v = +13.5$. In practice, the limiting detectable magnitude will be less than this since we have not taken into account atmospheric absorption, tracking jitter, non-statistical fluctuations, etc. This estimate of the idealized detector channel sensitivity is thus in fair agreement with the measured value.

5 Results

5.1 PULSE SHAPE

A total of 2222 events were identified as coming from meteors. Some examples of the types of pulses recorded are shown in Fig. 3. Because of the limited field of view of the detector, in general, these light pulses are only a portion of the meteor light curve. The rise and fall is dictated by the geometry of the detection system rather than the meteor physics.

The distribution of pulse widths is shown in Fig. 4; pulse width is defined as the full width at half maximum (FWHM). More than half the events recorded have pulse widths less than 20 ms. A meteor with a velocity of 40 km s^{-1} and horizontal trajectory at an altitude of 90 km would have a pulse width of 37 ms if it crossed the full 1° beam of the detector. The widths are therefore consistent with sporadic meteors traversing the detector beam at various angles and velocities. Only 16 events had widths of 0.4 s or greater.

The resolution of the system was limited by the chart recorder response, rather than the bandwidth of the electronics. It was not possible to resolve features of duration less than 20 ms.

If the pulse shapes are dominated by geometric effects, then it would be expected that the rise and fall times would be symmetrical. In practice, the amplifier response is such that the fall is slightly slower than the rise for a delta function input. When the events are sorted as to whether the rise time is greater than the fall time or vice versa, it is found that for pulse widths less than 100 ms, most of the pulses are symmetric (within the resolution of the analysis i.e. 20 ms) and that there is a tendency for pulse fall times to be longer than the rise times.

For pulse widths greater than 100 ms, the effect is quite different. 159 pulses have slower rise times compared with 94 which have slower fall times.

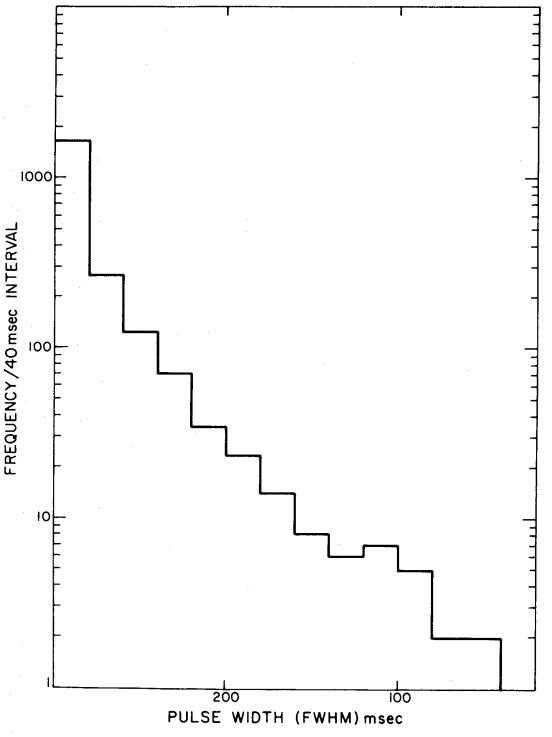

Figure 4. The distribution of pulse widths with time (FWHM).

Cook, Williams & Shao [5] have presented the light curves of 29 faint meteors which have a variety of shapes but show a characteristic rapid rise and slower fall. However, these meteors had a peak brightness in the range +6 to −1 with widths 0.4 to 1.2 s.

5.2 PULSE HEIGHT DISTRIBUTION

A pulse height distribution for all 2222 meteors recorded is plotted in Fig.4. The distribution is consistent with a power law of the form $N(>h) = kh^{-\gamma}$ where k is a constant and $\gamma = 1.33$. The range of pulse heights covered is 10^2, corresponding to a range of +12.0 to +7.0 m_{pg}. There is no evidence from the shapes of the pulses for saturation at the brigher end of the spectrum.

The data have also been divided by day and the exponents for the different days derived. The flattest distribution is found on December 14, but the observations of December 13 show a flat component at +9.0 m_{pg}.

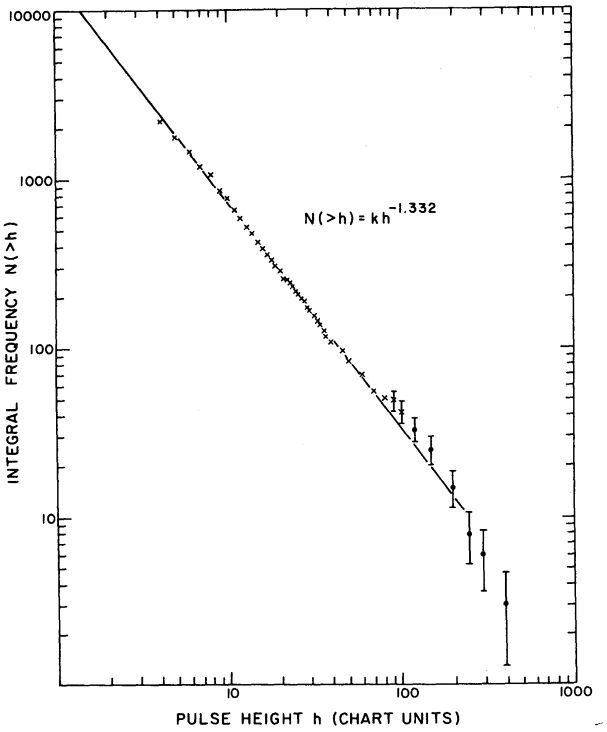

Figure 5. Integral pulse height distribution of all the recorded meteors in the detector channel A.

5.3 DIURNAL VARIATION

The observations exhibited the well-known diurnal variation in rate of arrival of meteors.

5.4 GUARD RING

Because of the lower relative efficiency of the guard ring, detector events that were near threshold ($h < 20$) had no counterpart in the guard ring; of the 319 detector pulses with $h > 20$, 67 per cent had no corresponding guard ring event. At very high thresholds ($h > 80$)

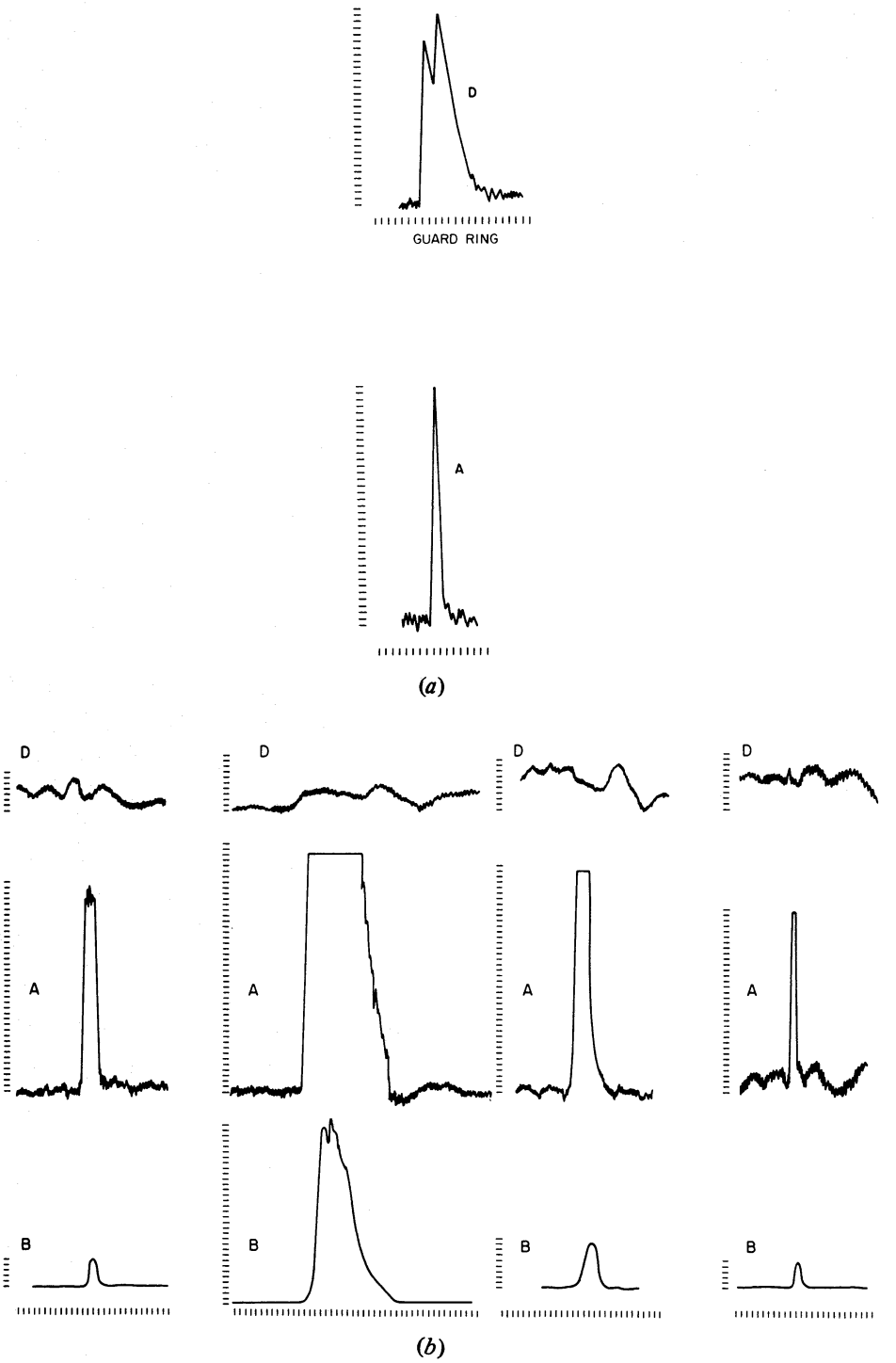

Figure 6. Large events in detector, channel A and guard ring, channel D. (a) Typical transverse meteor which was detected on either side of the detector (b) four bright meteors which had virtually no counterpart in the guard ring.

four of the 54 events had no guard ring event. For these events at least it would seem that the meteor trajectory was along the detector axis; thus the recorded light curve is most probably a true representation of the meteor light curve. These curves are shown in Fig. 6. The reader will note the absence of any suggestion of saturation in the brightest of these four meteors.

6 Discussion

GEMINID CONTRIBUTION

A feature of the rate of all events versus time is that there is no apparent difference between the rates on the four nights of observations. There is thus no evidence for a component from the Geminid shower (which was the original purpose of the observations). We conclude that the Geminid contribution at very faint luminosities is small compared with the sporadic contribution. (The alternative explanation that the Geminid shower did not show a significant variation over the four days, can be discounted since the growth and decay was seen at brighter luminosities during the same shower (Clifton, private communication).)

SPORADICS

The majority of the data comes from sporadics which transverse the beam of the detector at arbitrary angles. Because of the narrow beamwidth, these meteors will be only partially observed; the degree to which they are observed depends on the track length. From the observations of Jones & Hawkés [6] who used a single station TV system with a threshold of $+8\,m_{pg}$, a vertical track length of 5.7 km was deduced. This did not appear to change with luminosity. Since the geometric diameter of our beam at 90 km is 1.5 km, the detector will typically see only 25 per cent of the meteroid trail.

However, if the meteor light curve does not change its shape with luminosity, then a random sampling of sections of the light curve (i.e. light pulses above a certain theshold) will have the same pulse height distribution as the frequency – maximum luminosity distribution. (This argument is the same as that used to derive the primary cosmic ray spectrum from the observed Cerenkov light pulse spectrum from air showers where it is assumed that the lateral distribution of light does not change with energy i.e. the shape of the resulting light pulse distribution is independent of energy. Here the argument is stronger since a comparatively large fraction of the light distribution is sampled.)

At an altitude of 90 km the detector beamwidth has a radius of 0.75 km. The geometric collection area is then $\pi(0.75)^2\,\mathrm{km}^2$; however, since the track length is larger than the average chord intercepted by the meteor, the effective collection area is $3\,\mathrm{km}^2$ which is consistent with a track length of 3–6 km taking into account the variation in sensitivity of the tube across the field.

With this area and the observed detection rate of 2–6 meteor min^{-1}, we get a rate of 1.1 to 3.3×10^{-12} meteor $\mathrm{cm}^{-2}\,\mathrm{s}^{-1}$. Since the threshold $+12.0\,m_{pg}$ and the spectral index is 1.33, the meteroid spectrum can be fitted by a power law:

$$N(>h) = 3.3\times10^{-12}(h-h_0)^{-1.33}$$

or in terms of stellar magnitude

$$\log\phi = -11.48 + 0.533\,(m_{pg}-12.0) \qquad (1)$$

where the meteroid flux ϕ is in $\mathrm{cm}^{-2}\,\mathrm{s}^{-1}$.

The relatively simple experiments described here have shown that with a large optical reflector it is possible to detect meteors as faint as $+12\,m_{pg}$. The data obtained are limited by the lack of spatial resolution in the detectors which limits the interpretation of individual events. A Vidicon type system with its wide field and spatial resolution does allow the observation of light curves of individual meteors with certainty; it is, however, limited in its sensitivity and has many calibration problems.

A significant improvement in the system used here would be the utilization of a large array of smaller phototubes in the focal plane of the 10-m reflector. Since the resolution of the reflector is 0°.4 (5 cm in the focal plane) the ideal detection element is a phototube with 5 cm photocathode. Allowing 6 cm diameter for each phototube assembly, a total of 91 tubes could be fitted in a circle of diameter 75 cm (6°). Given the short track length of faint meteors, this system could totally observe the light curves of meteors as faint as $+13\,m_{pg}$ at a rate of 10–50 min^{-1}. Since the tubes have a wide dynamic range and could have their individual gains calibrated, detailed information on this difficult part of the meteor distribution spectrum would then become available. A somewhat similar system has been proposed for further work on gamma ray astronomy [7].

OTHER OBSERVATIONS

Apart from photoelectric and photographic techniques, ground-based methods to establish statistics of meteors have used either visual or radar meteor observations. There are severe difficulties with selection effects for both of these. The visual meteors require corrections for missed meteors all the way down from absolute magnitude zero (standard range for absolute magnitude is 100 km) as discussed by Hawkins & Upton [1]. Furthermore, for meteors brighter than absolute magnitude zero the visual scale becomes very uncertain owing to the absence of comparison stars. The radar meteors suffer from losses at the low velocity end [8, 9]. The ones at high velocities are missed because very rapid diffusion of the ionized trails takes place at the greater heights at which they occur. The lowest velocity radar meteors are missed on account of rapid dissociative recombination of molecular oxygen ions [9].

The only observations not beset with these difficulties are those of photographic meteors as reported by Hawkins & Upton [1], of faint television meteors by Hawkes & Jones [10] and those of very faint meteors reported in this paper. The magnitude ranges of the statistics are −2.4 to +1.6, 0 to +3 and +7 to +12 respectively (photographic absolute magnitudes). Clifton [11] has counted television meteors to varying threshold limits for stars seen in his field but has not determined the magnitudes of his individual meteors. His observations cover the magnitude range +3 to +8 and thus bridge the gap between our observations and those of Hawkes & Jones [10]. We regard these data as being so much better in quality than the old statistics of visual and radar meteors that we base our discussion solely on them. For a survey of the visual and radar statistics the reader is referred to the review article by Hughes [8].

INTERIM FIT TO HAWKINS & UPTON [1] AND TO OURSELVES

We wish to make an interim fit to the two sets of data at the extremes of the magnitude range available and then to investigate the deviations from that fit in the mid-range as they may be exhibited by the other observations.

We combine the present results with counts of photographic meteors versus maximum absolute photographic magnitude by Hawkins & Upton [1] to establish a tentative distribution over a wide range of magnitudes.

Hawkins & Upton [1] find a mean flux, ϕ, given by

$$\log \phi = -4.33 + 0.537\,M_{pg}$$

where ϕ is the cumulative flux on to the Earth's atmosphere in $km^{-2}\,hr^{-1}$ for meteors at or brighter than absolute photographic magnitude, M_{pg} (standard range 100 km), at maximum

brightness. We convert the flux to $cm^{-2}\ s^{-1}$ to find

$$\log \phi = -17.89 + 0.537 M_{pg}.$$

Our results may be put in the form

$$\log \phi = -17.88 + 0.533 M_{pg}.$$

The uncertainty of this observation is about ±0.4 in the logarithm but the slope is only uncertain by about ±0.004. The difference between apparent magnitude and absolute magnitude (standard range 100 km) has been neglected in this instance because the conversion from mean range to standard range must involve a factor much closer to unity than the largest and smallest corresponding to the overall uncertainty and because the effects of changing zenith distance (volume of meteor layer observed $\sim \sec^3 Z_R$, counting rate $\sim \cos^{2.66} Z_R$, combined effect $\sim \sec^{0.34} Z_R$, where Z_R denotes the zenith distance of the line-of-sight) are small.

The observations of Hawkins & Upton give complete counts over the range from $M_{pg} = -2.4$ to $M_{pg} = +1.6$. At the mid-point of this range we find $M_{pg} = -0.4$, $\log \phi = -18.10$. From the present data we have $M_{pg} = +12.0$, $\log \phi = -7.48$. A linear fit through these two points is

$$\log \phi = -17.89 + 0.534 M_{pg} \qquad (2)$$

which we adopt for comparison with the other two papers and indeed shall adopt as our final result. The slopes from the two sets of observations agree accurately. The agreement in constants is remarkable and fortuitous. We have thus adopted the common slope found by us and by Hawkins & Upton [1], to establish the zero point of our cumulative flux distribution. We must test this interpolation across the gap in photographic absolute magnitude from +1.6 to +7.0. We shall do so by comparison with the observations of Hawkes & Jones [10] and Clifton [11].

COMPARISON WITH HAWKES & JONES [10]

Hawkes & Jones [10] find for the flux in $m^{-2}\ s^{-1}$

$$\log \phi = -13.00 + 0.4\,(M_V - 2.5)$$

where M_V is the visual absolute magnitude at maximum brightness and the counts are complete in the range of M_V from +1 to +4. Application of a colour index of −1.0 [12] and conversion to flux in $cm^{-2}\ s^{-1}$ yields

$$\log \phi^* = -17.00 + 0.4\,(M_{pg} - 1.5).$$

The disagreement in slope over so short a range as 3 mag is unimportant. We find residuals at $M_{pg} = 0$ and +3 to compare with our fit as follows:

M_{pg}	$\log \phi^*$ (Hawkes & Jones)	$\log \phi$ (this paper)	$\log \phi^* - \log \phi$
0	−17.60	−17.89	+0.29
+3	−16.40	−16.29	−0.11

The mean residual at $M_{pg} = +1.5$ is +0.09 and this must be regarded as a satisfactory fit.

COMPARISON WITH CLIFTON [11]

Clifton's [11] observations cover a range in M_{pg} from +3 to +8 so that the entire range of magnitude covered by photographic, television and photoelectric observations runs from −2.4 to +12.0 for M_{pg}. His counts are in terms of threshold magnitudes of stars. He did not determine the magnitudes of individual meteors. Writing speed depends upon velocity so that the counts are in terms of mean values of $(M_{pg} - 2.5 \log V)$ rather than of M_{pg} alone. We can compare these counts with the others only by way of a discussion of the statistical distribution over velocity and of the effective lengths of the light curves. The luminosities per unit mass of meteors are involved in such a discussion whence it follows that we must invoke all the considerations needed to find the flux at a particular mass of meteoroid and larger.

Clifton states that he saw all meteors brighter than $M_{pg} = +6.4$, half of those at +8.1 and none at or fainter than +9.0 during operation in his system's mode of maximum sensitivity. The threshold for stars was at magnitude, $M_T = +11.0$ at zero colour index. We fit a visibility factor, f_v, of the form

$$\left.\begin{aligned} f_v &= 7.365\,(10^{-0.4 M_{pg}} - 0.0002512)^{1/3} \\ \log f_v &= 0.867 + 1/3 \log (10^{-0.4 M_{pg}} - 10^{-3.6}) \end{aligned}\right\} + 6.4 \leqslant M_{pg} \leqslant +9.0,$$

$$f_v = 1 \qquad M_{pg} \leqslant +6.4$$

$$f_v = 0 \qquad M_{pg} \geqslant +9.0.$$

We multiply the visibility factor against the differential distribution. We write the flux in the form

$$\log \phi = \log \phi\,(+6.4) + 0.5008\,(M_{pg} - 6.4)$$

using Clifton's slope. We convert to intensity,

$$I_{pg} = 10^{-0.4 M_{pg}}$$

and find

$$\phi = 10^{-3.20}\,\phi\,(+6.4)\,I_{pg}^{-1.252}$$

$$\phi' = \frac{d\phi}{dI_{pg}} = -7.81 \times 10^{-4}\,\phi\,(+6.4)\,I_{pg}^{-2.252}.$$

We then integrate over I_{pg} from $10^{-3.6}$ to $10^{-2.56}$ (i.e. from $M_{pg} = +9.0$ to $M_{pg} = +6.4$) to find the apparent flux at $M_{pg} = +9.0$,

$$\phi_{app}(+9.0) = \phi\,(+6.4) + 7.81 \times 10^{-4}\,\phi\,(+6.4) \int_{10^{-3.6}}^{10^{-2.56}} I_{pg}^{-2.252}\, f_v\, dI_{pg},$$

$$f_v = 7.365\,(I_{pg} - 0.0002512)^{1/3}.$$

A change of variable,

$$u \equiv 10^{+1.2}\,(I_{pg} - 0.0002512)^{1/3}$$

yields

$$\phi_{app}(+9.0) = \phi(+6.4)\left[1 + 34.99\int_0^{2.152}\frac{u^3 du}{(1+u^3)^{2.252}}\right].$$

Evaluation of the integral by numerical quadratures yields

$$\phi_{app}(+9.0) = 1.293\,\phi(+6.4) = \phi(+8.3).$$

This effective cut-off magnitude for Clifton's counts applies at the mean velocity of Clifton's meteors. Photographic meteors exhibit the same dependence of detection threshold on velocity and their mean velocity is 35.3 km s^{-1} [13]. The cut-off lies at

$$M_{pg} - 2.5\log\left(\frac{V}{\bar{V}}\right) = +8.3, \qquad \bar{V} = 35.3\,\text{km s}^{-1}$$

for Clifton's observations.

We pass from visibility of meteors to their luminosity. We begin with a discussion of luminous efficiency. The luminous efficiency, τ_{pg}, of a meteor in photographic light is customarily defined by the relation,

$$I_{pg} = \frac{\tau_{pg}}{2}\left(-\frac{dm}{dt}\right)V^2, \quad I_{pg} = 10^{-0.4 M_{pg}} \tag{3}$$

where I_{pg} is the instantaneous photographic brightness of the meteor, M_{pg} is its instantaneous photographic absolute magnitude, m is its mass, $-dm/dt$ is the rate of ablation of mass from the meteoroid and V is its velocity. It is evident that the right-hand side of the first equation is simply the product of the rate of deposit of kinetic energy of ablated mass from a meteor and the luminous efficiency which is the conversion factor from rate of deposit of kinetic energy to brightness of the meteor. The second equation is simply the standard relation for brightness to absolute magnitude. A similar relation applies for the luminous efficiency τ_v, of a meteor in visual light. We shall consider two conditions under which the radiation may be produced. The first is free molecular flow for which the relevant luminous efficiencies have been measured for iron [14, 15], sodium, calcium and magnesium [15]. Table 1 lists the adopted luminous efficiencies from these sources for meteoric stone with the standard composition introduced by Öpik [16, p. 160].

The other case, which may apply to meteoroids ablating by vaporization, is that of slip flow in a meteoroid's own vapours accompanied by free molecular flow relative to the air. This is Öpik's [16, Table VI, p. 139] compact coma while free molecular flow corresponds to his very dilute coma (loc. cit.). We form the ratios from these two cases from Öpik's calculations and apply them as conversion factors from free molecular flow to slip flow in its own vapours. Unfortunately the ratios are for visual luminous efficiencies but we apply them to photographic luminous efficiencies. Only the dominance of iron-radiations through much of the spectrum permits us to do so at all. This is so because the relative distribution of radiation across the near ultraviolet and visible range for iron is not sensitive to velocity [14]. These results are also listed in Table 1.

We can only continue toward a fit of Clifton's observations by invoking general considerations applicable to conversion from magnitudes to masses for all the observations.

The first step in passing from cumulative fluxes in terms of absolute magnitude to those in terms of mass or to cumulative number densities is to find the total light from the meteor

Table 1. Luminous efficiencies employed in this study.

Velocity, V (km s^{-1})	Free molecular flow, (0 mag g^{-1} cm^{-2} s^3 $\times 10^{-13}$)	Slip flow, τ_{pg} (0 mag g^{-1} cm^{-2} s^3 $\times 10^{-13}$)
11	1.9	1.6
12	2.2	2.1
14	2.6	2.8
16	2.7	3.2
18	2.8	3.6
20	2.6	3.8
22	2.4	4.0
24	2.3	4.3
26	2.2	4.6
28	2.1	4.9
30	2.0	5.3
32	1.8	5.4
34	1.7	5.8
36	1.7	6.1
38	1.6	6.4
40	1.6	6.6
42	1.5	6.9
44	1.5	6.7
46	1.3	6.6
48	1.2	6.5
50	1.1	6.3
55	0.95	6.0
60	0.80	5.6
65	0.72	5.1
70	0.65	4.5
72	0.55	4.3

in terms of its maximum brightness. We define an effective scale length of the light curve, H^*, as

$$H^* = \frac{V}{I_{pg\,max}} \int_{-\infty}^{+\infty} I_{pg}\, dt$$

where $I_{pg\,max}$ is the maximum brightness of the meteor. Levin [17, p. 101 equation 3.29] has defined μ via

$$\frac{A}{A_\infty} = \left(\frac{m}{m_\infty}\right)^{\mu}$$

where A is the presentation area of a meteoroid of mass, m, and the subscript ∞ denotes values before entry into the Earth's atmosphere. In the special case of unchanging spherical shape we have $\mu = 2/3$. This special case is that of the classical theory of a single meteoroid. Values of $\mu < 2/3$ provide empirical ways of allowing for progressive fragmentation in the context of Levin's treatment of the subject. Levin's [17, pp. 101–104, 120–121, 125, 127] analysis leads us to the expression

$$\frac{H}{\mu^{\mu/(1-\mu)} \cos Z_R} = \frac{V}{I_{pg\,max}} \int_{-\infty}^{+\infty} I_{pg}\, dt$$

where H is the local scale height in the terrestrial atmosphere and Z_R is the zenith distance of the meteor's radiant. Evidently we have

$$H^* = \frac{H}{\mu^{\mu/(1-\mu)} \cos Z_R}.$$

Levin [17, pp. 141–143] has discussed 140 super-Schmidt meteors reported by Hawkins & Southworth [13]. His table of the distribution versus μ can be transformed to a distribution versus $\mu^{\mu/(1-\mu)}$. We then find

$$\overline{\mu^{\mu/(1-\mu)}} = 0.58.$$

The mean value of $\cos Z_R$ over the sky is

$$\overline{\cos Z_R} = \frac{2\pi \int_0^{\pi/2} \sin Z_R \cos^2 Z_R \, dZ_R}{2\pi \int_0^{\pi/2} \sin Z_R \cos Z_R \, dZ_R} = 2/3.$$

Combination of this result with $H = 7.0$ km, a representative value, yields

$$H^* = 2.57\,H = 18.1 \text{ km}.$$

An alternative source of information is a discussion of 29 television meteors by Cook *et al.* [18]. Thirteen of the meteors had integrals over their light curves which could be measured and were judged to be better than very uncertain. The results are

$$\overline{\cos Z_R} = 0.677,$$

$$\frac{V \cos Z_R}{I_{pg\,max}} \int_{-\infty}^{+\infty} I \, dt = 10.2 \text{ km}.$$

The latter may be combined with $\overline{\cos Z_R} = 2/3$ to find

$$H^* \simeq 15.3 \text{ km}.$$

We adopt $H^* = 17$ km. The corresponding value for $\mu = 2/3$ or the so-called classical value is $H^* = 23.6$ km. Evidently the well-known shortness of the light curves shows here. This difference is generally believed to be due to progressive fragmentation of the meteoroids. Eight of the meteors reported by Cook *et al.* [18] had their light curves considerably shortened by their nearness to threshold, thus giving the appearance of even more shortness.

The next step is to alter the distribution of meteors over velocity appropriate for Clifton's observations (counts to levels of $I_{pg\,max}/V$) to that appropriate for all the other observations (counts to levels of $I_{pg\,max}$). The best distribution of meteors versus velocity for counts to levels of $I_{pg\,max}/V$ is that for super-Schmidt meteors by Hawkins & Southworth [13]. The distribution need only by multiplied by $(V/\bar{V})^\alpha$ where $\alpha = 1.335$ (corresponding to our adopted distribution, the coefficient of M_{pg} is 0.4α). Of course, the new distribution must be re-normalized. A result is a new mean velocity, $\bar{V}^*$,

$$\bar{V}^* = 45.6 \text{ km s}^{-1}.$$

The old distribution is denoted by $f(V)$, the new distribution by $f^*(V)$ where we recall that the old mean velocity, $\bar{V}$, is

$$\bar{V} = 35.3 \text{ km s}^{-1}.$$

We now introduce as a reference mass that of a zeroth magnitude meteor at $V = \bar{V}$. The mass of a meteoroid is given by solution of equation (3) for dm/dt and integration

$$m_\infty = \frac{2}{\tau V^2}\int_{-\infty}^{+\infty} I_{pg}\, dt = \frac{2H^*}{\tau V^3} I_{pg\,max} \tag{4}$$

if we neglect the change of velocity along the trajectory. At $V = \bar{V}$ a zeroth magnitude meteor will have the mass

$$m_{\infty 0} = \frac{2H^*}{\tau \bar{V}^3} = \frac{2H^*}{\tau \bar{V}^2}\frac{1}{\bar{V}} \tag{5}$$

and if we reduce the contributions of the counts to this velocity we have an integral of the form

$$\int_{V_1}^{V_2} \frac{f(V)[2H^*/(\tau V^2 \bar{V})]^\alpha\, dV}{[2H^*/(\tau \bar{V}^3)]^\alpha} = \int_{V_1}^{V_2} f(V)\left[\frac{\tau(\bar{V})}{\tau(V)}\left(\frac{\bar{V}}{V}\right)^2\right]^\alpha dV \tag{6}$$

where V_1, V_2 are the lower and upper limits of velocities of meteors outside the atmosphere. This integral is appropriate for Clifton's observations. For all the other observations the appropriate integral is

$$\int_{V_1}^{V_2} \frac{f(V)[2H^*/(\tau V^3)]^\alpha}{[2H^*/(\tau V^{*3}]^\alpha} dt = \int_{V_1}^{V_2} f^*(V)\left[\frac{\tau(V^*)}{\tau(V)}\left(\frac{V^*}{V}\right)^3\right]^\alpha dV. \tag{7}$$

In free molecular flow the two integrals take the values 1.72, 3.18 respectively and in slip flow in the meteor's own vapours they take the values 4.89 and 14.7. The logarithms of the ratios in these two cases are +0.27 and +0.48. These correspond to shifts in meteor magnitude of −0.5 and −0.9 respectively (on division by 0.534). Application of these to the +8.3 mag counting limit leads to the conclusion that Clifton's total counts are valid to M_{pg} = +7.8 if the meteors are in free molecular flow or to M_{pg} = +7.4 if the meteors are in slip flow of their own vapours. His total count as a function of magnitude of the threshold stars, M_T is

$$\log \phi = -15.294 + 0.5008\, M_T$$

for counts in $m^{-2}\, s^{-1}$ and hence

$$\log \phi = -19.294 + 0.5008\, M_T$$

for counts in $cm^{-2}\, s^{-1}$. The threshold magnitude corresponding to the above two meteor magnitudes is +11.0 whence

$$\log \phi = -13.785.$$

Our adopted formula yields

M_{pg}	$\log \phi$	Residual (Clifton minus fit)
+7.8	−13.72	−0.06
+7.4	−13.94	+0.16

Since Clifton's counts cover some five magnitudes we find for five magnitudes brighter a count

$$\log \phi = 16.29.$$

At this brightness our interim formula yields

M_{pg}	$\log \phi$	Residual (Clifton minus fit)
+2.8	−16.39	+0.10
+2.4	−16.61	−0.32

The mean residual for free molecular flow is +0.02 and for slip flow in own vapours is +0.24. Accordingly we treat them as favouring free molecular flow and adopt

M_{pg}	$\log \phi$	Residual (Clifton minus fit)
+2.8	−16.29	+0.10
+7.8	−13.78	−0.06

Finally we adopt

$$\log \phi = -17.89 + 0.534\, M_{pg}. \quad (8)$$

Fig. 7 displays our adopted fit and the trends found from Hawkes & Jones [10] and Clifton [11]. We refrain from cluttering this display with the traditional lines from visual meteors and radar meteors (see, e.g. [8]) which will lie lower because of observational selection already mentioned.

We have reached a remarkable and unexpected result. The single slope all the way from photographic absolute magnitude −2.4 to +12.0 appears to be confirmed by the observations of Hawkes & Jones and supported by those of Clifton. Indeed, if we were to insist on the model of slip flow of a meteoroid in its own vapours we would find an interval of steeper slope at intermediate magnitudes and then recalibrate our observations to still higher

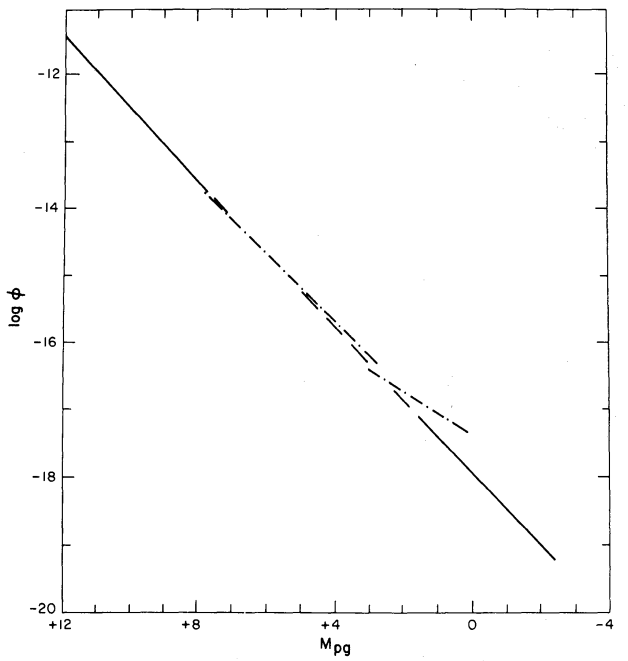

Figure 7. Logarithm of cumulative flux ($cm^{-2}\, s^{-1}$) of sporadic meteors upon the Earth's atmosphere versus photographic absolute magnitude. Solid lines denote the results of Hawkins & Upton [1] and ourselves fitted in zero point to Hawkins & Upton. The dashed line in between is our adopted fit. The lower dash dotted line displays the results of Hawkes & Jones [10] while the upper one exhibits those of Clifton [11] with our calibration of his observations. The flux is intended to be an average over all zenith directions.

levels. This contrasts with the customary view that the slope steadily decreases as fainter meteors are considered (see, e.g. [8, 19]).

CONVERSION TO CUMULATIVE FLUXES VERSUS MASS AT THE EARTH'S ATMOSPHERE AND FAR FROM THE EARTH

The coefficient of M_{pg} in equation (8) is to be multiplied by ~ 2.5 to pass to one for the logarithm of the mass. From equations (5) and (6) the constant is to be increased by

$$\log\left\{\left(\frac{2H^*}{\tau\bar{V}^{*3}}\right)^{\alpha}\int_{V_1}^{V_2} f^*(V)\left[\frac{\tau(\bar{V}^*)}{\tau(V)}\left(\frac{\bar{V}}{V}\right)^3\right]^{\alpha} dV\right\} =$$

$$\log\left\{\int_{V_1}^{V_2} f^*(V)\left[\left(\frac{2H^*}{\tau V^3}\right)^{\alpha} dV\right]\right\} = -0.24$$

found by numerical quadratures, whence we find

$$\log \phi_{m\infty} = -18.13 - 1.335 \log m_{\infty}$$

where $\phi_{m\infty}$ is the cumulative flux in $cm^{-2}\,s^{-1}$ upon the atmosphere of meteoroids of mass equal to or greater than m_{∞}. For slip flow in own vapours the constant becomes -18.41.

An alternative procedure is to use the velocity distribution at constant m_{∞} deduced from radar meteors by Southworth & Sekanina [9]. We denote the relative distribution over velocity by f^{**} and seek the average luminosity per gram

$$I_{pg\,0} = \frac{\int_{V_1}^{V_2} f^{**}(V)\,\tau_{pg}(V)\,V^3\,dV}{2H^{*\alpha}\int_{V_1}^{V_2} f^{**}(V)\,dV},$$

$$= 0.284\,0 \text{ mag g}^{-1}$$

found by numerical quadratures. The reduction to be applied to the constant in our formula is

$$-1.335 \log I_{pg\,0} = +0.73$$

whence we find

$$\log \phi_{m\infty} = -17.16 - 1.335 \log m_{\infty}.$$

The corresponding value of $I_{pg\,0}$ for slip flow in own vapours is 0.496 0 mag s^{-1}, of -1.335 $\log I_{pg\,0}$ is $+0.41$ and of the constant in the above expression is -17.48. It seems best to adopt a mean formula,

$$\log \phi_{m\infty} = -17.80 - 1.335 \log m_{\infty}. \qquad (9)$$
$$\pm 0.62 \pm 0.010$$

We desire the average flux on a test surface at 1 AU from the Sun and far from the Earth's gravitational field. The optical observations call for a ratio of fluxes

$$\frac{\phi_{mG}}{\phi_{m\infty}} = \frac{\int_{V_1}^{V_2} f^*(V)[2H^*/(\tau V^3)]^{\alpha}(V_G/V)^2\, dV}{\int_{V_1}^{V_2} f^*(V)[2H^*/(\tau V^3)]^{\alpha}\, dV}$$

$$V_G = (V^2 - V_{es}^2)^{1/2},$$

$$V_{es}^2 = 1.234 \times 10^{12}\ \mathrm{cm^2\ s^{-2}}$$

where V_G is the geocentric velocity of the meteor, V_{es} is the velocity of escape from the Earth at meteoric heights and ϕ_{mG} is the flux at 1 AU from the Sun outside the Earth's gravitational field. The weighting factor is described by Levin [17, p. 210, equation 5.7]. Numerical quadratures yield

$$\log(\phi_{mG}/\phi_{m\infty}) = -0.17, \qquad \log \phi_{mG} = -18.30 - 1.335 \log m_\infty.$$

In slip flow in own vapours the constant becomes −18.58.

From the radar meteors the same ratio may be written

$$\frac{\phi_{mG}}{\phi_{m\infty}} = \frac{\int_{V_1}^{V_2} f^{**}(V)\,(V_G/V)^2\, dV}{\int_{V_1}^{V_2} f^{**}(V)\, dV}.$$

Numerical quadratures yield

$$\log(\phi_{mG}/\phi_{m\infty}) = -0.66, \qquad \log \phi_{mG} = -17.82 - 1.335 \log m_\infty.$$

In slip flow in own vapours the constant becomes −18.14. The difference is due to the much stronger statistical role of slow meteors in the very abundant radar data. Again we adopt the mean to find

$$\log \phi_{mG} = \underset{\pm 0.38}{-18.21} \underset{\pm 0.010}{-1.335} \log m_\infty. \qquad (10)$$

NUMBER DENSITY OF METEOROIDS AT 1 AU FROM THE SUN

The cumulative number of meteoroids per $\mathrm{cm^3}$ of mass larger than or equal to a given mass of meteoroids, m_∞, is also an objective of these statistical observations. We require representative values of V_G both for the optical and the radar meteors. These may be obtained from the formula [17, p. 210, equation 5.7],

$$\frac{\phi_{mG}}{\phi_{m\infty}} = \left(\frac{V_G}{V}\right)^2 = \frac{V_G^2}{V_G^2 + V_{es}^2}$$

for a given velocity. From the optical observations we find $16.0\ \mathrm{km\ s^{-1}}$ and from the radar meteor distribution we find $5.9\ \mathrm{km\ s^{-1}}$.

The ratio of the number density of meteoroids as a function of mass at 1 AU from the Sun and far from the Earth's gravitation to the flux on the Earth's atmosphere may be expressed for the optical observations as

$$\frac{N_{\mathrm{mG}}}{\phi_{\mathrm{m}\infty}} = \frac{\int_{V_1}^{V_2} f(V)\,[2H^*/(\tau V^3)]^{\alpha}(4V_{\mathrm{G}}/V^2)\,dV}{\int_{V_1}^{V_2} f^{**}(V)[2H^*/(\tau V^3)]^{\alpha}\,dV}$$

where the factor 4 comes from the ratio of the area of an entire sphere to that of its cross-section. The symbol, N_{mG}, denotes the number of meteoroids per cm^3 of mass m_∞ or greater. The logarithm of this ratio may be had from numerical quadratures and is

$$\log (N_{\mathrm{mG}}/\phi_{\mathrm{m}\infty}) = -6.05.$$

The corresponding cumulative number density is

$$\log N_{\mathrm{mG}} = -24.35 - 1.335 \log m_\infty.$$

in free molecular flow. The constant is -24.63 for slip flow in own vapours. An average velocity may be found from

$$\bar{V}_{\mathrm{G}} = \frac{4\phi_{\mathrm{mG}}}{N_{\mathrm{mG}}} = 18.3 \text{ km s}^{-1}.$$

The corresponding average velocity appropriate to the radar meteor distribution may be scaled in the ratio of the two representative values already found above (5.9 and 16.0 km s^{-1}) whence we adopt

$$\bar{V}_{\mathrm{G}} = 6.8 \text{ km s}^{-1}$$

$$\log (N_{\mathrm{mG}}) = -5.23, \qquad \log N_{\mathrm{mG}} = -23.05 - 1.335 \log m_\infty,$$

in free molecular flow. The constant becomes -23.37 if slip flow in own vapours prevails. We adopt the mean

$$\log N_{\mathrm{mG}} = -23.8 - 1.335 \log m_\infty. \qquad (11)$$
$$\pm 0.8 \quad \pm 0.010$$

This is our final result, valid in the range of logarithm of mass

$$-4.4 \leqslant \log m_\infty \leqslant +1.4 \qquad (12)$$

corresponding to $+12.0 \leqslant M_{\mathrm{pg}} \leqslant -2.4$. The uncertainty in the mass scale is about ± 0.5 in the logarithm. It is dominated by the uncertainty in the distribution over velocity.

DISCUSSION

It should be apparent to the reader that the accuracy of the successive results declines from being rather good for equation (2) for the total flux versus threshold absolute magnitude to less certain for equation (9) for the total flux versus threshold mass (which is affected by composition, luminous efficiency and velocity distribution) to still more uncertain for equation (10) for the total flux versus threshold mass at 1 AU from the Sun but far from the Earth (which is strongly affected by the velocity distribution). Finally equation (11) for the cumulative number per unit volume versus threshold mass is still more affected by the

velocity distribution and must be the least accurate of all our results. The formal uncertainty estimated in that equation is probably rather optimistic. It should also be noted that approximately half of the meteors photographed by super-Schmidt cameras can be grouped into well defined streams [20, 21] while only 7.5 per cent of faint radar meteors can be grouped even into doubtful poorly defined streams [22]. The implied more rapid evolution of the smaller meteoroids also implies an altered distribution over direction and velocity at the Earth so that for statistics in terms of a cut-off mass the 'constants' used above may be larger for smaller masses. The observational data for meteors are insufficient to permit a satisfactory discussion at present. In any event the above treatment in terms of velocity distributions is a much needed replacement for the old habit of using an arbitrary representative velocity [23].

We should like to close by quoting a memorable sentence in Leinert's [19] review article on the zodiacal light: 'Vielleicht ist die Struktur der interplanetaren Staubwolke doch wesentlicher komplizierter, als es nach Zodiakallicht-Beobachtungen das Anschein hat.' We can only add: for 'Zodiakallicht-Beobachtungen' read 'Meteor-Beobachtungen'!

Acknowledgements

We are grateful to E. Horine for assistance during the observations and to G. Harney who performed the preliminary data analysis. This work was supported by NASA under contract No. NSG-8024.

References

[1] Hawkins, G. S. & Upton, E. K. L., 1958. *Astrophys. J.*, **128**, 727.
[2] Weekes, T. C., Fazio, G. G., Helmken, H. F., O'Mongain, E. & Rieke, G. H., 1972. *Astrophys. J.*, **174**, 165.
[3] Clifton, K. L., 1973. *J. geophys. Res.*, **73**, 6511.
[4] Allen, C. W., 1973. *Astrophysical Quantities*, Athlone Press, London.
[5] Cook, A. F., Williams, J. T. & Shao, C. Y., 1973. In *Evolution and Physical Properties of Meteoroids* p. 23, ed. Hemenway, C. L., Millman, P. M. & Cook, A. F., NASA SP-319.
[6] Jones, J. & Hawkes, R. L., 1975. *Mon. Not. R. astr. Soc.*, **171**, 159.
[7] Weekes, T. C. & Turver, K. E., 1977. *Proceedings of the 12th ESLAB Symposium on Gamma Ray Astronomy*, p. 279, Frascati, Italy May 1977.
[8] Hughes, D. W., 1975. In *Space Research XV*, p. 531, ed. Rycroft, M. J., Akademie-Verlag, Berlin.
[9] Southworth, R. B. & Sekanina, Z., 1973. *Physical and Dynamical Studies of Meteors*, NASA CR-2316.
[10] Hawkes, R. L. & Jones, 1975. *Mon. Not. R. astr. Soc.*, **170**, 363.
[11] Clifton K. S., 1973. *J. geophys. Res.*, **73**, 6511.
[12] Jacchia, L. G., 1957. *Astr. J.*, **62**, 358.
[13] Hawkins, G. S. & Southworth, R. B., 1958. *Smithson. Contr. Astrophys.*, **2**, 349.
[14] Friichtenicht, J. F. & Becker, D. G., 1973. In *Evolutionary and Physical Properties of Meteoroids*, p. 53, ed. Hemenway, C. L., Millman, P. M. & Cook, A. F., NASA SP-319.
[15] Savage, H. F. & Boitnott, C. S., 1973. In *Evolutionary and Physical Properties of Meteoroids*, p. 83, ed. Hemenway, C. L., Millman, P. M. & Cook, A. F., NASA SP-319.
[16] Öpik, E. J., 1958. *Physics of Meteor Flight in the Atmosphere*, Interscience, New York.
[17] Levin, B. J., 1961. *Physikalische Theorie der Meteore und die meteoritische Substanz im Sonnensystem*, ed. Richter, N., Akademie-Verlag, Berlin.
[18] Cook, A. F., Forti, G., McCrosky, R. E., Posen, A., Southworth, R. B. & Williams, J. T., 1973. In *Evolutionary and Physical Properties of Meteors*, p. 23, ed. Hemenway, C. L., Millman, P. M. & Cook, A. F., NASA SP-319.
[19] Leinert, C., 1979. *Naturewiss.* **221**, 66.
[20] McCrosky, R. E. & Posen, A., 1961. *Smithson. Contr. Astrophys.*, **4**, 15.
[21] Cook, A. F., 1973. In *Evolutionary and Physical Properties of Meteoroids*, p. 183, ed. Hemenway, C. L., Millman, P. M. & Cook, A. F., NASA SP-319.
[22] Sekanina, Z., 1973. *Icarus*, **18**, 253.
[23] Verniani, F., 1973. *J. geophys. Res.*, **78**, 8429.